Journal of Thermal Analysis and Calorimetry, Vol. 89 (2007) 2, 479–490

A COMPARISON OF ISOCONVERSIONAL AND MODEL-FITTING APPROACHES TO KINETIC PARAMETER ESTIMATION AND APPLICATION PREDICTIONS

A. K. Burnham[*] *and L. N. Dinh*

P. O. Box 808, Lawrence Livermore National Laboratory, Livermore, CA 94551, USA

A variety of isoconversional and model fitting approaches, all of which use multiple heating schedules, are used to analyze selected data from the ICTAC kinetics and lifetime projects as well as additional simulated data sets created for this work. The objective is to compare the accuracy and suitability of various approaches for various types of chemical reactions. The various simulated data sets show that model fitting and isoconversional methods have comparable reliability for extrapolation outside the range of calibration. First, there is as much variability in prediction for various isoconversional methods as there is between isoconversional methods as a group and different plausible explicit models. Of the three isoconversional models investigated, the Friedman method is usually the most accurate. This is particularly true for energetic materials that have a drop in apparent activation energy in the latter stages of reaction, which leads to a delayed onset of rapid autocatalysis at lower temperatures. It is difficult to determine a priori whether isoconversional or model fitting approaches will give more accurate predictions. The greatest reliability is attained by using both the isoconversional and model fitting approaches on a combination of isothermal and constant heating rate data.

Keywords: *ICTAC, isoconversional kinetics, kinetic models, model fitting*

Introduction

Chemical kinetic modeling has been used for many years in process optimization, estimating real-time material performance, and lifetime prediction. Chemists have tended towards developing detailed mechanistic models, while engineers have tended towards global or lumped models. Many, if not most, applications use global models by necessity, since it is impractical or impossible to develop a rigorous mechanistic model. Model fitting acquired a bad connotation in the thermal analysis community after that community realized a decade after other disciplines that deriving kinetic parameters for an assumed model from a single heating rate produced unreliable and sometimes nonsensical results. In its place, advanced isoconversional methods [1], which have their roots in the Friedman [2] and Ozawa–Flynn–Wall [3] methods of the 1960's, have become increasingly popular. In fact, as pointed out by the ICTAC kinetics project in 2000 [4, 5], both isoconversional and model fitting methods can be used beneficially as long as a diverse set of heating schedules are used to derive the kinetic parameters. The current paper extends the understanding from that project to give a better appreciation of the strengths and weaknesses of isoconversional and model-fitting approaches. Examples are given from a variety of sources, including the former and current ICTAC round-robin exercises, data sets for materials of interest, and simulated data sets.

Kinetic models

A common starting point for kinetic analysis within the thermal analysis community is

$$\frac{\mathrm{d}\alpha}{\mathrm{d}t} = kf(\alpha) = A\mathrm{e}^{-\frac{E}{RT}} f(\alpha) \qquad (1)$$

where α is the fraction converted, t is time, $f(\alpha)$ is a reaction model, and $k=A\exp(-E/RT)$, where A is the frequency factor, E is the activation energy, R is the gas constant, and T is temperature. Both the LLNL Kinetics05 [6] and AKTS Thermokinetics programs [7] use the Friedman isoconversional method [2], in which an Arrhenius plot of the instantaneous rate, in units of fraction reacted per unit time, is made at each selected α for experiments with different thermal histories:

$$\ln\left(\frac{\mathrm{d}\alpha}{\mathrm{d}t_\alpha}\right) = -\frac{E_\alpha}{RT_\alpha} + \ln\{A_\alpha f(\alpha)\} \qquad (2)$$

where t_α, T_α, E_α and A_α are the time, temperature, apparent activation energy and pre-exponential factor, respectively, at conversion α. $-E_\alpha/R$ and $\ln\{A_\alpha f(\alpha)\}$

---

[*] Author for correspondence: burnham1@llnl.gov

1388–6150/$20.00

Akadémiai Kiadó, Budapest, Hungary
Springer, Dordrecht, The Netherlands

are the slope and the intercept with the vertical axis of the plot of $\ln(d\alpha/dt_\alpha)$ *vs.* $1/T_\alpha$.

It is also possible to make kinetic predictions at any temperature, T_0, directly from the values of E_α and $\{A_\alpha f(\alpha)\}$ extracted directly from the Friedman method by separation of like terms in Eq. (1) followed by integration:

$$t_\alpha = \int_0^{t_\alpha} dt = \int_0^{\alpha} \frac{d\alpha}{\{A_\alpha f(\alpha)\} e^{-\frac{E_\alpha}{RT_0}}} \tag{3}$$

No specification of the reaction model term, $f(\alpha)$, is necessary in the kinetic prediction since only the product term, $\{A_\alpha f(\alpha)\}$, which is experimentally extracted from the kinetic experiment according to Eq. (2), is needed in the kinetic prediction Eq. (3) along with E_α. Equations (2) and (3) form the complete foundation for all of the Friedman isoconversional kinetic measurements and predictions presented in this report. However, nothing can be inferred about the pre-exponential factor, A_α, unless $f(\alpha)$ takes on some particular form (first-order reaction, nucleation-growth, etc.). And when $f(\alpha)$ is associated with a specific reaction model, the experimentally extracted product term, $\{A_\alpha f(\alpha)\}$, still remains unchanged, hence the kinetic prediction also remains unchanged and A_α is constrained to take on only values determined by the product term, $\{A_\alpha f(\alpha)\}$. LLNL Kinetics05 takes advantage of this unique property of the Friedman isoconversional kinetic measurement and prediction to probe the magnitude and variation of the apparent first-order pre-exponential factor, A_α. This is a convenient way of displaying the result and does not imply a specific mechanism.

Alternately, with β as the heating rate, Eq. (1) can be rewritten as:

$$g(\alpha) = \int_0^{\alpha} \frac{d\alpha}{f(\alpha)} = \int_0^{T_\alpha} \frac{A}{\beta} \exp\left(-\frac{E}{RT}\right) dT \tag{4}$$

In the notation of $x \equiv E/RT$, Eq. (4) becomes:

$$\beta \frac{R}{AE} \int_0^{\alpha} \frac{d\alpha}{f(\alpha)} = \int_x^{\infty} x^{-2} \exp(-x) dx \tag{5}$$

The right hand side of Eq. (5) is also known as the temperature integral, $p(x)$, which has no analytical solution in closed form but can be approximated.

The Kissinger–Akahira–Sunose (KAS) method adopts the approximation:

$$p(x) \cong \exp(-x)/x^2 \ (20<x<50) \tag{6}$$

The KAS approximation shown in Eq. (6) is possible only with the assumption of a constant activation energy from the beginning of the reaction to the conversion level α of interest.

Substituting Eq. (6) into Eq. (5) yields:

$$\ln\left(\frac{\beta}{T_\alpha^2}\right) \cong -\frac{E}{R}\left(\frac{1}{T_\alpha}\right) - \ln\left\{\left(\frac{E}{AR}\right) \int_0^{\alpha} \frac{d\alpha}{f(\alpha)}\right\} \tag{7}$$

Equation (7) is known as the KAS integral isoconversional method [8].

The Ozawa–Flynn–Wall (OFW) method takes another approximation:

$$p(x) \cong \exp(-1.052x - 5.33) \ (20<x<60) \tag{8}$$

Like the KAS approximation, the OFW approximation shown in Eq. (8) assumes a constant activation energy from the beginning of the reaction to the conversion level α of interest.

Substituting Eq. (8) into Eq. (5) yields:

$$ln(\beta) = -1.052\frac{E}{R}\left(\frac{1}{T_\alpha}\right) - 5.33 - \ln\left\{\left(\frac{R}{AE}\right) \int_0^{\alpha} \frac{d\alpha}{f(\alpha)}\right\} \tag{9}$$

Equation (9) is known as the OFW integral isoconversional method [3, 9–11].

The KAS and OFW methods were originally derived for processes with constant activation energies. And hence, the errors associated with kinetic measurements from the KAS and OFW methods should be dependent on the magnitude of the variation of the activation energy with respect to α. For any process involving a variation in the kinetic parameters with respect to the conversion level, the KAS and OFW methods approximate E and A in the temperature integral from $\alpha=0$ to the conversion level of interest with an apparent constant activation energy, $\overline{E}_\alpha$, and an apparent constant pre-exponential factor, $\overline{A}_\alpha$. So when the activation energy changes with the reacted fraction, Eqs (7) and (9) can be more meaningfully written as:

$$\ln\left(\frac{\beta}{T_\alpha^2}\right) \cong -\frac{\overline{E}_\alpha}{R}\left(\frac{1}{T_\alpha}\right) - \ln\left\{\left(\frac{\overline{E}_\alpha}{\overline{A}_\alpha R}\right) \int_0^{\alpha} \frac{d\alpha}{f(\alpha)}\right\} \tag{10}$$

(KAS)

$$\ln(\beta) \cong -1.052\frac{\overline{E}_\alpha}{R}\left(\frac{1}{T_\alpha}\right) - 5.33 - \ln\left\{\left(\frac{R}{\overline{A}_\alpha \overline{E}_\alpha}\right) \int_0^{\alpha} \frac{d\alpha}{f(\alpha)}\right\} \tag{11}$$

(OFW)

Due to the mathematical forms of the KAS and OFW methods, the only kinetic parameter that can be easily extracted is the activation energy. Kinetic predictions from the KAS and OFW are, however, possible through the use of an approximation proposed by Vyazovkin [12]. In this approximation, the $g(\alpha)$ expression for the isothermal condition (at T_0) is equated with the corresponding one for the non-isothermal condition to yield:

$$t_\alpha = \left[\beta e^{-\frac{E_\alpha}{RT_0}}\right]^{-1} \int_0^{T_\alpha} e^{-\frac{E_\alpha}{RT}} dT \qquad (12)$$

Vyazovkin's time prediction above assumes the conservation of the kinetic parameters when changing temperature at the conversion level of interest [12]. The thermal integral in Eq. (12) should be approximated with KAS approximation (Eq. (6)) and OFW approximation (Eq. (8)) to make kinetic predictions for the kinetic measurements obtained from the KAS method (Eq. (10)) and OFW method (Eq. (11)), respectively. The kinetic predictions appropriate for the kinetic parameters obtained from the KAS and OFW methods are, therefore:

$$t_\alpha = \left[\beta e^{-\frac{\bar{E}_\alpha}{RT_0}}\right]^{-1} \left[\frac{RT_\alpha^2}{\bar{E}_\alpha}\right] \exp\left(-\frac{\bar{E}_\alpha}{RT_\alpha}\right) \qquad (13)$$

(for kinetics from KAS method)

$$t_\alpha = \left[\beta e^{-\frac{\bar{E}_\alpha}{RT_0}}\right]^{-1} \left(\frac{\bar{E}_\alpha}{R}\right) \exp\left(-\frac{1.052\bar{E}_\alpha}{RT_\alpha} - 5.33\right) \qquad (14)$$

(for kinetics from OFW method)

The KAS and OFW methods are not included in Kinetics05 but were implemented in a separate computer program. This program also included Friedman's method, and calculations with this program agreed well with Kinetics05 even though slightly different numerical integration algorithms were used.

An often-useful kinetic model in Kinetics05 is an extended Prout-Tompkins (nucleation-growth) model [13]:

$$\frac{d\alpha}{dt} = k(1-\alpha)^n (1-q(1-\alpha))^m \qquad (15)$$

where q is an initiation parameter and m is a parameter related to the growth dimensionality or branching ratio, depending on whether the reaction is a solid-state or fluid-state reaction. The parameter q is necessary for the reaction to have a non-zero reaction rate for $\alpha=0$, and earlier similar forms of Eq. (15), e.g., by Šesták and Berggren [14], implicitly include some way to get the reaction started. If $n=0$ and $m=1$, Eq. (15) has the limit of the linear chain-branching model. If $n=1$ and $m=0$, it has the limit of a first-order reaction. In $n=m=1$, it is the standard Prout–Tompkins model [15]. Kinetics05 has the ability to fit up to three parallel nucleation-growth reactions.

Kinetics05 has two other models that were used in this work. First, it can fit up to three parallel n^{th}-order reactions, each of which can have a Gaussian distribution of activation energies [16]. Second, it has the ability to fit up to 25 parallel first-order reactions by an iterative linear-nonlinear regression method [17]. For the latter, the A can be constant or it can follow the relationship $\ln(A)=A_0+\ln(E)$.

Another reaction model in Kinetics05 that was not used for fitting but was used to create simulated data is the alternate pathway model, in which components X, Y, and P have the following reaction pathways: X to Y, Y to P, and X to P. In each pathway, the rate constant is an nth-order reaction having a Gaussian distribution of activation energies, which gives a distribution of rate constants for each reaction.

Comparison using real data sets

Many kinetics applications have a complex set of source and sink terms linked to specific observables. Often, competitive processes are involved. One simple example involving thermal analysis is when both endotherms and exotherms occur during the breakdown of a given material. When the endotherms and exotherms are well separated, the data can be cut and fitted separately, but often they overlap. Thermo-

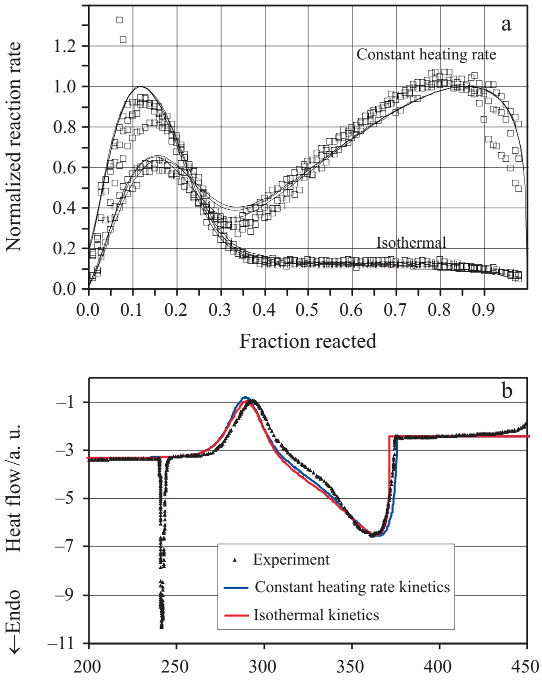

Fig. 1 a – Simultaneous fit (lines) of isothermal and constant heating rate TG data (points) for ammonium perchlorate to concurrent nucleation-growth and n^{th}-order reactions. The activation energies of the two reactions were 95.4 and 109.9 kJ mol^{-1}, respectively. b – Comparison of DSC data at 5°C min^{-1} (points) to calculations using kinetic parameters from independent fits to isothermal and nonisothermal TG data and independent enthalpies for endothermic evaporation and exothermic decomposition. No attempt was made to model the phase transition at 241°C

gravimetric data (TG) for ammonium perchlorate from the 2000 ICTAC kinetic study was fitted to two concurrent reactions, as shown in the top of Fig. 1. The faster process is endothermic, and the slower process is exothermic. By assigning enthalpies of different signs and recombining the reactions, one can simulate differential scanning calorimetry data (DSC) very well, as shown in the bottom of Fig. 1. This is not possible with an isoconversional model and demonstrates one potential advantage of a model-fitting approach.

The current ICTAC lifetime data sets (C. Popescu, organizer) have two energetic materials of particular interest, known as samples B3 and 4. Both these materials appear to be propellants. We present results for these in order to define a few reaction characteristics that are subsequently explored with simulated data sets. The Friedman isoconversional fit to the fraction of heat released from Sample B3, using a nonlinear baseline and Kinetics05, is shown in the top of Fig. 2. A corresponding fit to a reaction having three parallel nucleation-growth reactions is shown in the bottom of Fig. 2. The parallel reaction model parameters are shown in Table 1. The isoconversional fit is slightly better, but the differences are comparable to the degree that the reaction profiles change shape as a function of heating rate.

Table 1 Rate parameters for the model fit to Sample B3 data given in Fig. 2

Fraction	A/s^{-1}	E/kJ mol^{-1}	m	n
0.522	$1.65\cdot10^{16}$	160.96	0.60	2.0
0.231	$1.22\cdot10^{15}$	157.83	0.78	1.0
0.247	$6.41\cdot10^{15}$	198.13	0.00	2.4

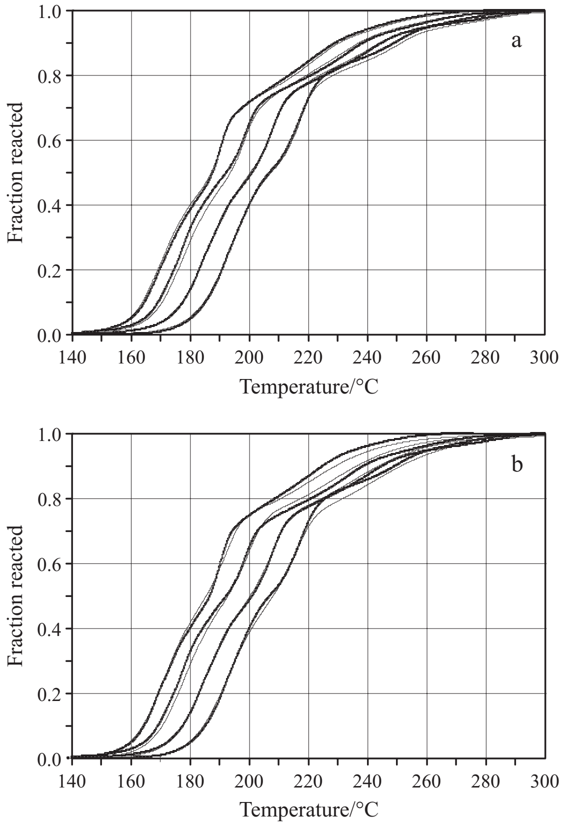

Fig. 2 Comparison of fits to ICTAC Sample B3 using a – Friedman isoconversional and b – parallel nucleation-growth models. The heating rates, from left to right, are 0.5, 1.0, 2.0, and 4.0°C min^{-1}

These data were also analyzed by the AKTS Thermokinetics program, which has a more sophisticated baseline optimization feature than Kinetics05. Even so, the results from that program are also affected by the baseline cutting procedure, and the kinetic parameters from two different cuts (labeled AKTS1 and AKTS2) are compared in the top of Fig. 3 to those from Kinetics05 using linear and nonlinear baseline corrections. An additional optimization by the AKTS code using the nonlinear baseline correction from Kinetics05 gave a very similar result to Kinetics05, so the leverage is in the baseline correction itself, not in other aspects of the optimization.

The corresponding predictions of the fraction reacted as a function of time are shown in the bottom of Fig. 3. The AKTS parameters predict a sooner reaction to half conversion, and this is a direct consequence of the lower activation energies in the 15–50% conversion range. All isoconversional models predict a sharp step in fraction converted sometime between 1 and 100 years. The fractional conversion at which this sharp step begins is related to where a dip in activation energy occurs. Similarly, the step stops at the conversion at which the activation energy rises again.

To the extent that this feature is real, it is difficult to mimic with more conventional modeling approaches. This is because isoconversional methods are really infinitely sequential models, which cannot be represented by a limited number of sequential reactions. A lower activation energy for the latter stages of reaction causes it to have a faster rate constant than the initial stage of reaction when temperature is decreased, so when it has the opportunity to occur at low temperature after the initial reactions are completed, it goes very rapidly.

It is interesting that the concurrent nucleation-growth reaction model tracks the isoconversional model derived from the same baseline correction up to 30% conversion, but it diverges by not predicting the substantial slowdown of the reaction at ~35% conversion. This is because the activation energy for the parallel reaction model does not increase until the

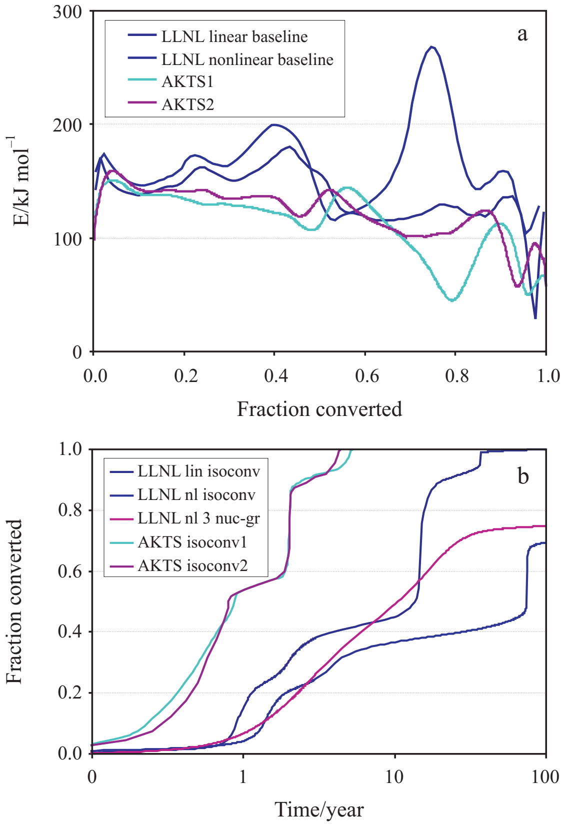

Fig. 3 a – Activation energy as a function of fraction converted for four separate Friedman isoconversional kinetic analyses of ICTAC Sample B3 using different baseline corrections, and b – predictions of the fraction converted *vs.* time at 80°C for those four kinetic models plus the parallel nucleation-growth model

last 25% of conversion, as shown in Table 1 and mirrored in the bottom of Fig. 3.

Kinetic models for sample 4 of the ICTAC data set yield a similar prediction of an induction time when the kinetics are extrapolated to lower temperature for a lifetime prediction. As a first step, the data can be fitted well with both isoconversional and parallel nucleation growth models, as shown in Fig. 4. The nucleation-growth model parameters are shown in Table 2, and the isoconversional *A* and *E* are shown in Fig. 5.

All three isoconversional models predict a substantial induction time for the subsequent rapid reaction from 50 to 100% conversion. The AKTS code predicts a longer induction time and starts the step at a higher conversion, which is a direct reflection of the higher peak E and higher conversion in Fig. 5. The two LLNL isoconversional parameter sets are for slightly different baseline corrections. The longer induction time predicted here by the AKTS code is just the opposite of shown in Fig. 3 for Sample B3. The parallel nucleation model also shows an acceleratory reaction characteristic, but the initial plateau is at

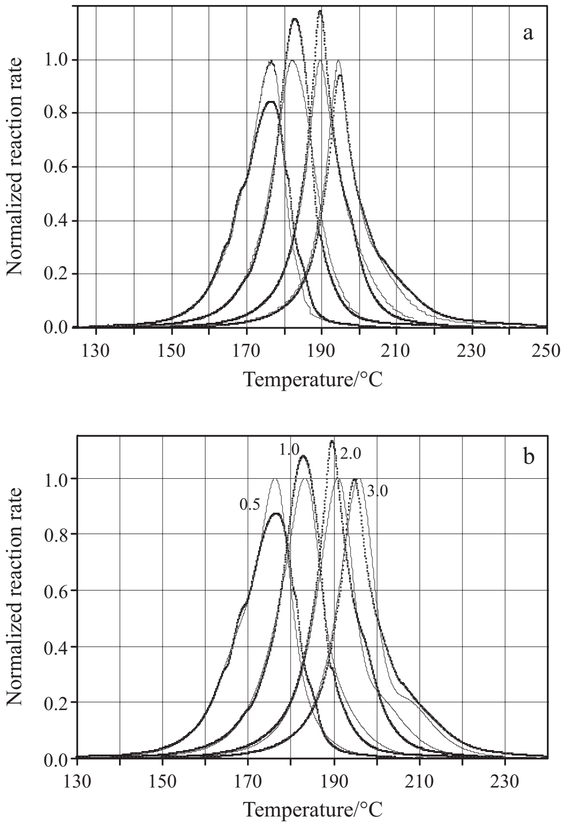

Fig. 4 Comparison of measured and calculated normalized heat flow from ICTAC Sample 4 for a – Friedman isoconversional and b – parallel nucleation-growth models. The heating rates, from left to right, are 0.5, 1.0, 2.0 and 3.0°C min^{-1}

Table 2 Rate parameters for the model fit to Sample 4 data given in Fig. 4b

Fraction	A/s^{-1}	E/kJ mol^{-1}	m	n
0.238	$3.79\cdot10^{9}$	103.63	0.82	0.76
0.493	$2.43\cdot10^{15}$	153.31	0.96	1.06
0.269	$6.41\cdot10^{15}$	110.49	0.93	1.38

higher conversion. That is because the second and third reactions have switched the order in which they occur – the 50% conversion plateau represents completion of reactions 1 and 3.

Figure 5 demonstrates two very important points about the relative merits of isoconversional and traditional model fitting: (1) the sequential reaction character of isoconversional modeling in combination with a higher activation energy in the middle conversion range leads to an induction time followed by a very rapid reaction; (2) the concurrent reaction model allows the order of the reaction to change if markedly different activation energies are involved and the higher temperature processes in the calibration set are associated with a low activation energy. Neither can be argued to be correct in the absence of other infor-

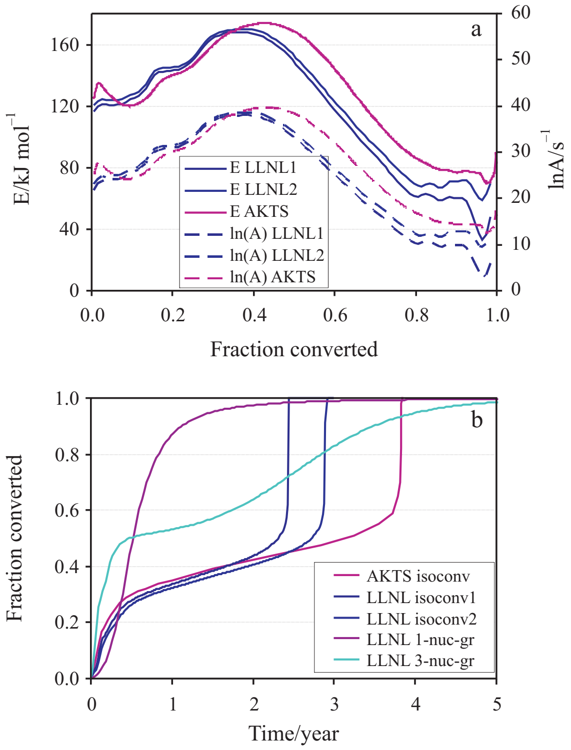

Fig. 5 a – Comparison of Friedman isoconversional kinetic parameters from various baseline correction attempts, and b – predictions of the resulting kinetic parameters for isothermal reaction at 80°C for ICTAC Sample 4

mation, e.g., isothermal experiments at about 160°C. Roduit *et al.* [18] have shown experimentally that propellants do tend to have a rapid decomposition after a long induction time at modest isothermal heating, so the isoconversional model predictions are plausible in this case. However, a conclusion that these predictions are suitable for propellants based on confirming evidence does not automatically mean they are suitable for other classes of materials.

Comparison using simulated data sets

The simulated data set in the 2000 ICTAC kinetics study consisted of two, equally weighted, parallel reactions with activation energies of 80 and 120 kJ mol^{-1} [4]. One of us (AB) was one of four participants that recovered the correct kinetic parameters. Isoconversional analysis gives an activation energy that gradually increases from the low 80 kJ mol^{-1} range to about 120 kJ mol^{-1}. Both methods gave good fits by any conventional standard, but the parallel reaction model had much smaller residuals than a real data set, as would be expected. The isoconversional fit is shown in the top of Fig. 6.

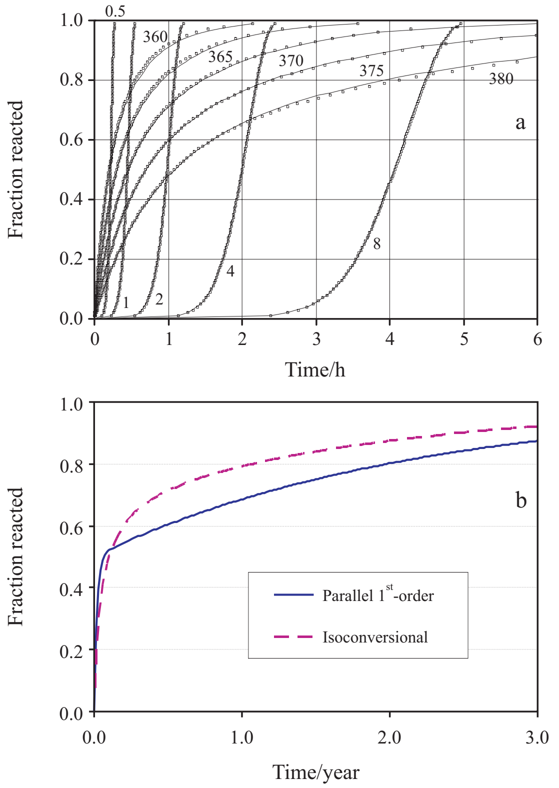

Fig. 6 a – Fit (lines) of the 2000 ICTAC simulated data (points) to a Friedman isoconversional model. Single digit numbers are the heating rates in °C min^{-1}, and triple digit numbers are isothermal temperatures in °C. b – A comparison of the prediction of that isoconversional model with the rigorous parallel reaction model at 25°C

The primary issue here is how well the parameters extrapolate outside the range of calibration. The parallel reaction model is compared to the isoconversional model in the bottom of Fig. 6 at a temperature of 25°C. Although the isoconversional model prediction is in the vicinity of the parallel reaction model, it misses the sharpness of the transition from the fast to the slow reaction in the simulation model, which is rigorously correct by definition. This is because the simulation model had been constructed so that the reactions overlap extensively at the calibration temperature interval, but they separate in proportion to the difference in temperature from the calibration interval.

The 2005 ICTAC lifetime-prediction study currently in progress contains one obviously simulated data set. A fit to an isoconversional model and the dependence of *E* and ln(*A*) on conversion are shown in Fig. 7. The steady increase in *E* with conversion means that a parallel reaction model should also work and give similar predictions. Fits to a discrete activation energy model [6] (i.e., a parallel reaction model commonly used in petroleum geochemistry having a set of evenly spaced activation energies and using the same frequency factor for all reactions) and to three concurrent nth-order reactions are shown in Fig. 8, and the kinetic parameters are shown in Table 3. The

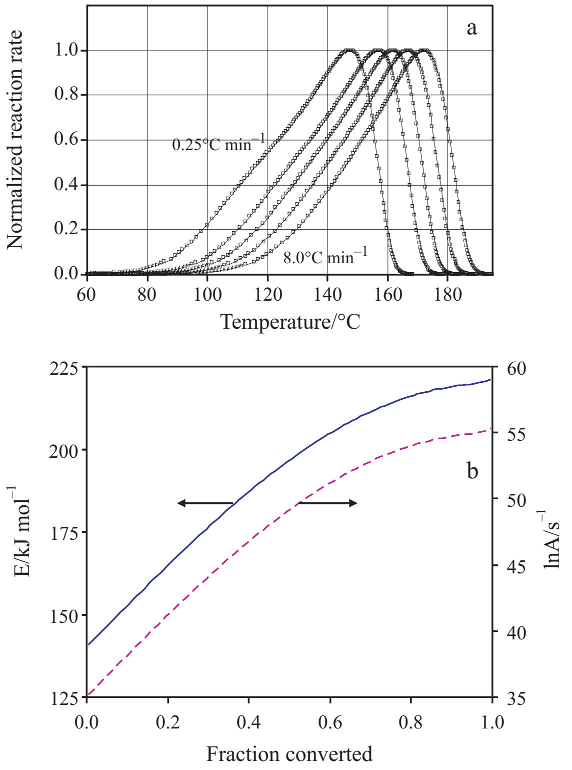

Fig. 7 a – Friedman isoconversional kinetic fit and b – kinetic parameters for the 2005 ICTAC simulated data set (Sample 1). The heating rates, from left to right, are 0.25, 1.0, 2.0, 4.0 and 8.0°C min^{-1}

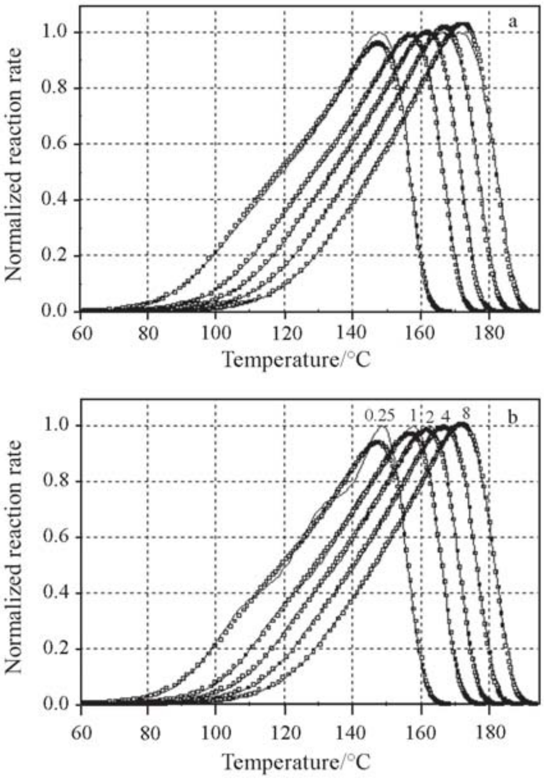

Fig. 8 Fits of the a – discrete activation energy and b – parallel n^{th}-order reaction models to the 2005 ICTAC simulated data set (Sample 1). The heating rates, from left to right, are 0.25, 1.0, 2.0, 4.0 and 8.0°C min^{-1}

Table 3 Rate parameters for the model fits to Sample 1 data shown in Fig. 8.

Parallel n^{th}-order reaction model

Fraction	A/s^{-1}	$E/\text{kJ mol}^{-1}$	n
0.192	$5.47\cdot10^{15}$	139.44	1.45
0.336	$1.64\cdot10^{18}$	166.10	1.31
0.472	$5.52\cdot10^{22}$	210.06	1.03

Discrete activation energy model

$\ln(A)=4.4841+0.2274\ E/\text{kJ mol}^{-1}$

Fraction	$E/\text{kJ mol}^{-1}$	Fraction	$E/\text{kJ mol}^{-1}$
0.0214	125.59	0.0802	167.51
0.0376	133.17	0.0527	176.10
0.0627	141.76	0.1495	184.69
0.0606	150.34	0.0552	201.86
0.0780	158.93	0.4021	210.45

highest energy reactions in both models have similar fractions and activation energies, and the isoconversional activation energy increases to 221.2 kJ mol^{-1} at high conversion.

Thermal histories prescribed by ICTAC for the lifetime prediction comparison are 3 years at 25, 50, and 80°C, and 3 years at 25 and 50°C with diurnal variations of 10 and 30°C, respectively. Predictions for these four fitting approaches to the Sample 1 data are given in Table 4. The predictions are very close to each other. How they compare to ground truth will be known when the generating model is released.

Three additional simulated data sets were created to further explore the reliability of isoconversional and parallel reaction models when reaction profiles change shape subtly as a function of heating rate. They are defined in Table 5. All involve the reaction of a starting material that does not contain visible

Table 4 Predictions of the four Sample 1 models for three years (%) at the specified temperatures (°C)

Model	25	50	80	25±10	50±30
Isoconversional	3.11	24.97	72.62	5.19	54.43
Discrete E distribution	4.51	24.80	70.43	6.49	52.95
3-parallel n^{th}-order	3.27	25.47	69.56	5.67	54.50

Table 5 Reaction parameters used to derive three additional sets of simulated data

Alternate Pathway Model

Reaction	A/s^{-1}	E/kJ mol^{-1}	σ/% of E	n
X→Y	$1.00\cdot10^{15}$	159.0	5.00	2.00
X→P	$1.00\cdot10^{12}$	125.5	0.00	1.00
Y→P	$4.00\cdot10^{15}$	159.0	0.00	2.00

Sequential Reaction Model I

Reaction	A/s^{-1}	E/kJ mol^{-1}
X→Y	$5.00\cdot10^{8}$	100.4
Y→0.3Z+0.7P	$4.00\cdot10^{9}$	108.8
0.3Z→0.3P	$5.00\cdot10^{6}$	92.0

Sequential Reaction Model II

Reaction	A/s^{-1}	E/kJ mol^{-1}
X→Y	$1.00\cdot10^{12}$	142.3
Y→0.3Z+0.7P	$4.00\cdot10^{9}$	108.8
0.3Z→0.3P	$3.00\cdot10^{4}$	75.3

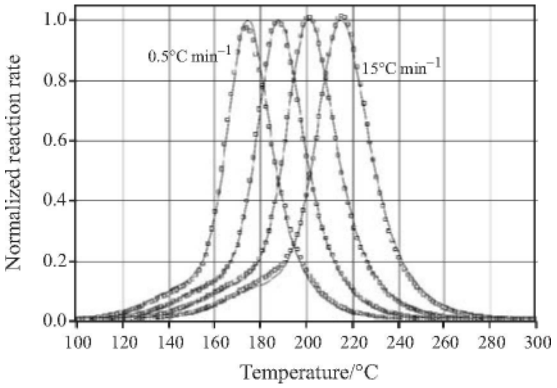

Fig. 9 Comparison of simulated data from the competing pathway model to a fit using two parallel nucleation-growth reactions. Heating rates, from left to right, are 0.5, 1.67, 5.0 and 15°C min^{-1}

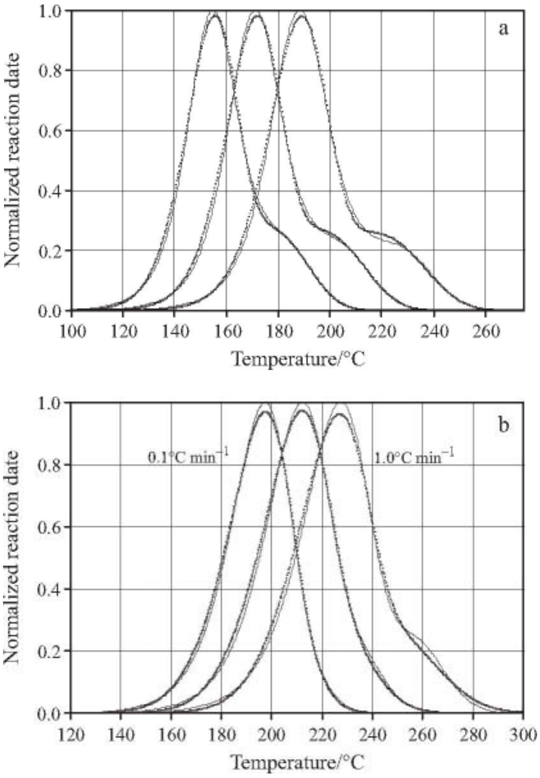

Fig. 10 Comparison of simulated Sequential Reaction Models a – I and b – II with fits to two parallel nucleation-growth models. Heating rates from left to right are 0.10, 0.32 and 1.0°C min^{-1}

Table 6 Rate parameters for the parallel nucleation-growth reaction model fits to the simulated data sets defined in Table 5

Fraction	A/s^{-1}	E/kJ mol^{-1}	m	n
Alternate Pathway Model				
0.102	$3.06\cdot10^{15}$	147.70	0.00	2.09
0.898	$1.16\cdot10^{14}$	144.63	0.55	2.02
Sequential Model I				
0.788	$1.76\cdot10^{9}$	105.02	0.59	1.46
0.212	$4.29\cdot10^{6}$	91.67	0.30	0.92
Sequential Model II				
0.772	$3.79\cdot10^{11}$	138.24	0.17	1.00
0.228	$3.53\cdot10^{6}$	94.77	0.54	1.05

product (P), and all generate visible product by two distinct routes. Fits to parallel nucleation growth models are shown in Figs 9 and 10 and the nucleation-growth parameters are in Table 6.

The Friedman isoconversional kinetic parameters for the three simulated data sets are shown in Fig. 11. As expected, the activation energy and frequency factor vary significantly in concert with conversion for each model. Qualitatively, conversion dependence can be related to differences in the activation energies in the simulating model. However, there are quantitative differences that can cause anomalous predictions. Predictions of the isoconversional and parallel nucleation-growth models are also shown in Fig. 11.

In the Alternate Pathway Model, the Friedman isoconversional approach works better, particularly below 25% conversion. Even so, the isoconversional prediction contains oscillations over this interval that appear to be related to the fact that the simulated data does not follow the isoconversional principle. This deviation contributes to the oscillation in activation energy in frequency factor below 20% conversion, which in turn, appears in the predicted conversion *vs.* time plot. The parallel nucleation-growth model does not have this oscillation problem, but its predicted reaction rate is too fast by a larger margin overall.

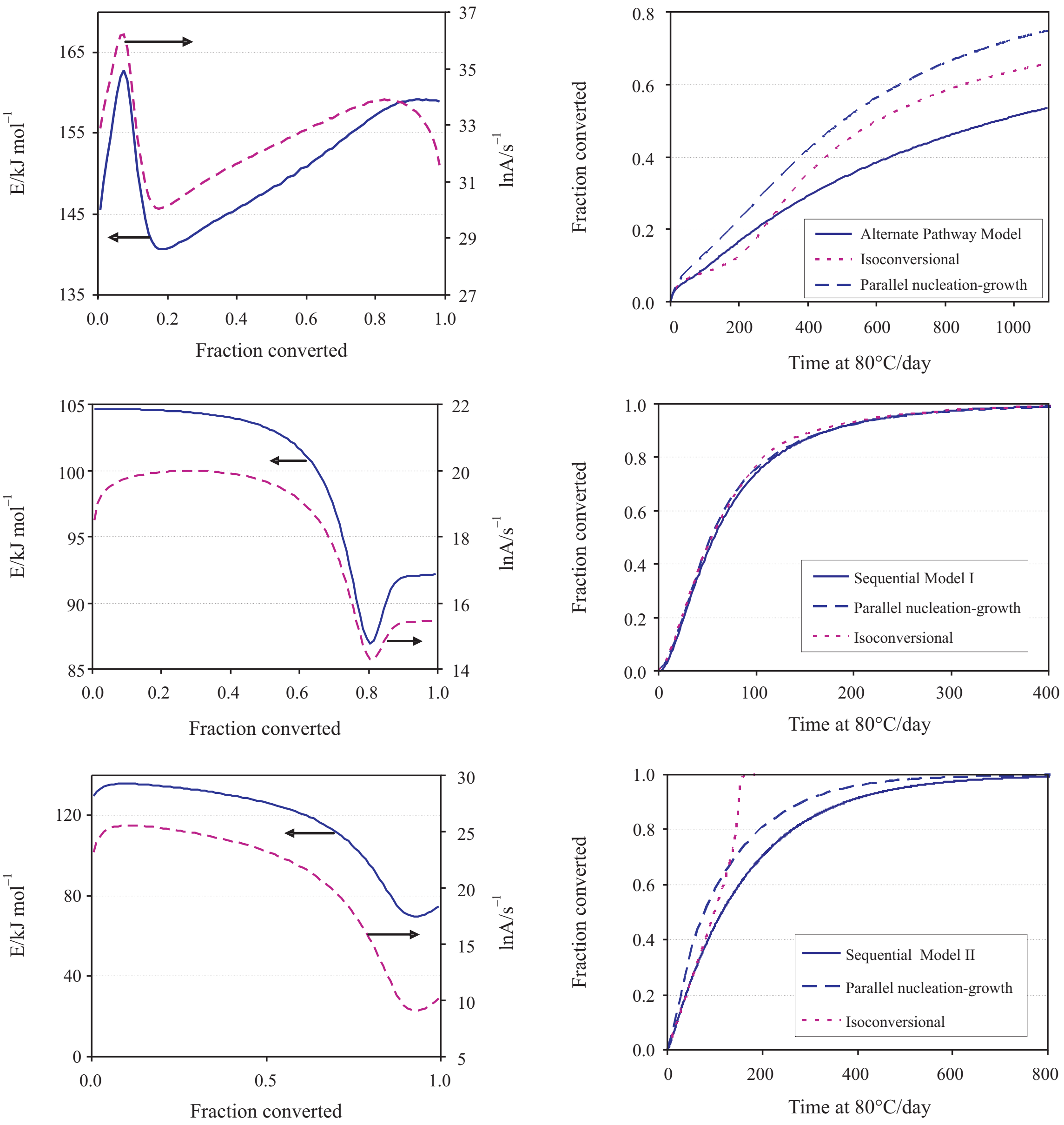

Fig. 11 Conversion-dependence of *A* and *E* (left) and comparison of the extrapolated Friedman isoconversional and parallel nucleation models to ground truth (right) for the three simulated data cases

Both the Friedman isoconversional and nucleation-growth models work very well for the Sequential Model I simulated data. Although not evident at the scale in Fig. 11, both underestimate the induction time over the first few days. Although the activation energy drops by about 18% in the Friedman model around 80% conversion, apparently such a drop is not large enough to cause a sharp increase in the reaction rates as seen in Figs 3 and 5. In contrast, the magnitude of drop in activation energy is larger in Sequential Model II, and the different characteristics of a few (true by definition here) and many (isoconversional assumption) sequential reactions causes the isoconversional model to falsely predict a kinetic runaway after 150 days. Consequently, although the isoconversional model does better for the first half of the reaction, the parallel nucleation-growth model does better for the second half of the reaction.

To this point, all isoconversional parameters have used the differential Friedman approach. The differential approach contains fewest assumptions of any isoconversional approach, as pointed out by Professor Ozawa in his 2006 NATAS award address.

The activation energies from the Table 5 simulated data sets are shown in Fig. 12 for the Friedman, OFW and KAS isoconversional approaches along with a comparison of the predictions of the three isoconversional methods to the ground-truth model calculation. Kinetic predictions presented in Fig. 12 were made with the help of Eqs (3), (13) and (14) for the Friedman, KAS and OFW methods, respectively. The differences among the isoconversional methods are striking. The OFW method tends to yield substantially higher activation energies relative to those in the model used to generate the simulated data, and, hence, tends to under-predict the fraction converted by a large margin. Since the KAS and OFW methods approximate the activation energy, *E,* in the temperature integral from α=0 to the conversion level of interest with an apparent constant activation energy, $\overline{E}_\alpha$, most of the bumps and sharp features in the Friedman activation energy plots tend to average out in the KAS and OFW methods. In the alternate pathway model, all three isoconversional methods have an artificial initial dip in the activation energy compared to the underlying model. In the sequential models, the Friedman model has an artificial dip at late conversion. Nevertheless, the kinetic prediction at 80°C from the Friedman and KAS methods are similar enough for the Alternate Pathway and Sequential Model I cases. For Sequential Model II, the Friedman method incorrectly predicts a run away reaction after a reacted fraction of about 0.4, but the two integral isoconversional

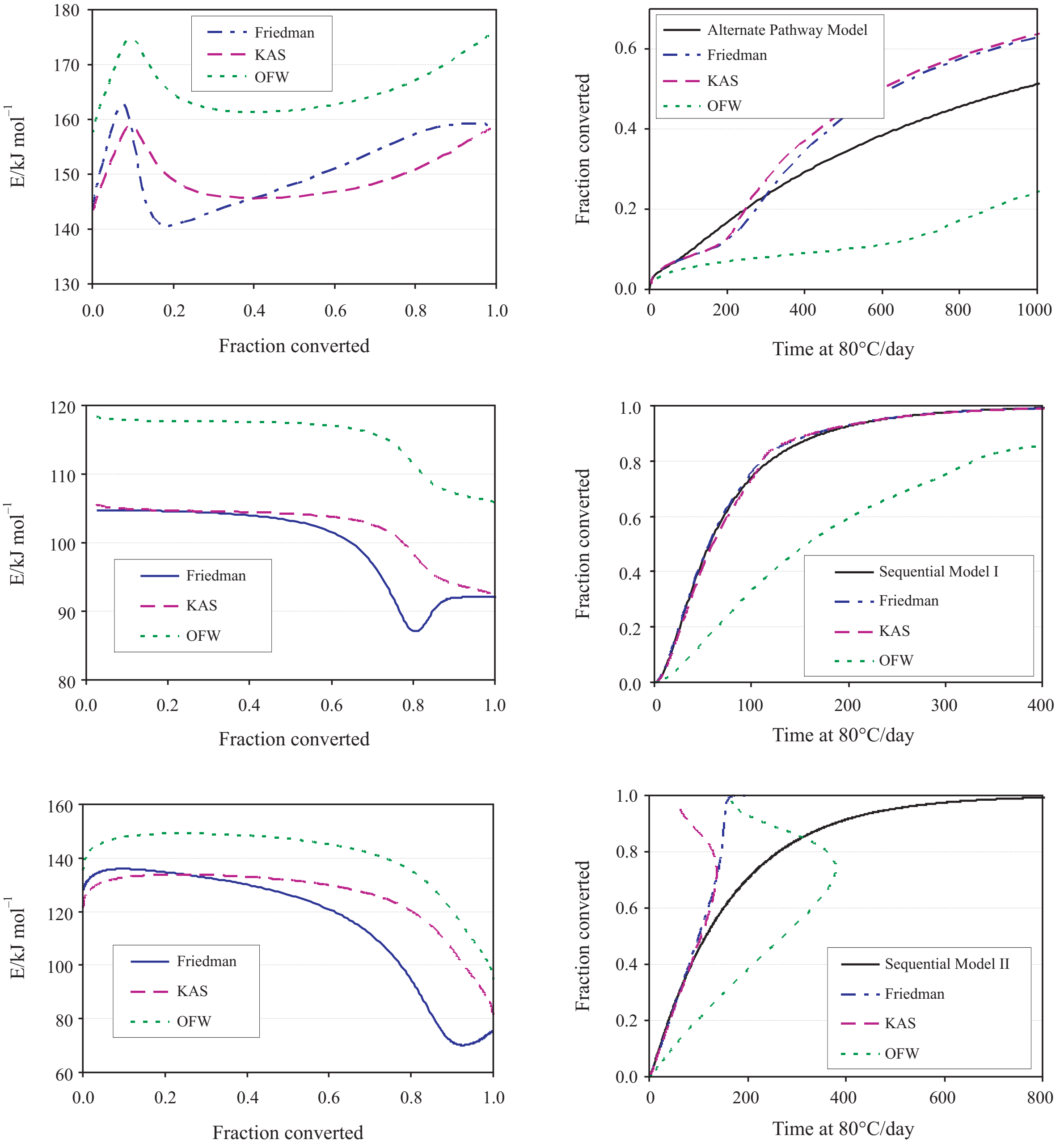

Fig. 12 Comparison of activation energies from the three different isoconversional methods and their predictions for the same ground truth simulations presented in Fig. 11

methods display a peculiar feature after a reacted fraction of about 0.75 in which less time is needed to reach $\alpha>0.75$ than to reach $\alpha=0.75$. This peculiar feature is a mathematical artifact since it is not present in the ground truth model or in the Friedman method. Indeed, this peculiar artifact can be traced back to the fact that the basic tenet for using Vyazovkin's kinetic prediction (Eq. (12)), namely the conservation of the kinetic parameters when changing temperature, does not hold well in the Sequential Model II at $\alpha>0.75$ where the activation energy decreases very fast with small increments in temperature.

In terms of the accuracies of the various isoconversional kinetic predictions, the Friedman method combined with Eq. (3) or the alternative approach employed in Kinetics05 comes the closest to the ground truth models in all cases. The susceptibility of the Friedman method to errors arising from experimental noise can be effectively mitigated if the rate of data recording during experiments is high so that the raw data can be significantly smoothed prior to the application of the derivative-based Friedman technique. So with proper smoothing of the data, the Friedman technique seems to be a reliable technique in all cases. Among the two integral isoconversional approaches investigated in this report, the kinetic measurements and predictions from the KAS method seem to be much more accurate than the OFW method, but less accurate than the derivative-based Friedman method. A similar conclusion has been reported by Starink [19] who attributes the poor accuracy of the OFW method to its crude approximation of the temperature integral. In addition, there is a need to replace the original temperature integral in the integral isoconversional approach with a series of finite integrations over smaller time intervals if the activation energy has a strong dependence on the fraction reacted [1]. In the limit of very small time interval, this advanced integral isoconversional approach converges to the results obtained from the Friedman technique [1] on simulated data.

Conclusions

Isoconversional methods are undoubtedly the quickest way to derive kinetic parameters for complex reaction profiles involving multiple processes. However, isoconversional methods, sometimes called 'model-free' kinetic analyses, are not assumption-free, and it is important to understand those assumptions and the limits they impose on predictions outside the range of calibration.

The essential characteristic of the Friedman (differential) isoconversional method is that it is an infinitely sequential model. The reaction profile changes shape as a function of temperature or heating rate by having different activation energies associated with different extents of conversion. Energetic materials appear to have reaction characteristics that are generally consistent with the isoconversional principle as long as the confinement conditions are constant and appropriate to the intended application.

Integral isoconversional methods are more complicated. The activation energy measured at each conversion is actually a result of approximating the activation energy of the conversion up to that point with a constant value. The KAS method uses a better approximation of the temperature integral and so is more accurate than the OFW method. But when the activation energy drops substantially in the later stages of conversion, both can give nonsensical kinetic predictions which violate the sequential reaction assumptions intrinsic to the models. However, many shortcomings associated with the integral isoconversional methods can be overcome by making the integral method piecewise continuous, which in the limit of small steps, makes it equivalent to the differential isoconversional method.

Despite the strengths and common utility of the differential and piecewise continuous integral isoconversional method, the isoconversional principle is fundamentally inapplicable to reaction networks having competing reactions, in which the ultimate outcome of the reaction can be different depending on the temperature as well as for concurrent reactions that change which one is faster over the temperature range of interest. Also, it is also not a good technique for sparse data sets or when the extent of conversion is incomplete and greatly different in different experiments, which is often the case with isothermal experiments.

Explicit models are potentially more flexible but suffer from issues of uniqueness. Explicit models can be either sequential or concurrent in nature, or any mixture thereof. Numerical integration techniques allow models of essentially any complexity to be used in an application mode, but unique calibration of many parameters by nonlinear regression becomes problematic without simplifying assumptions or independent experiments that emphasize or isolate different characteristics. If the reaction is fundamentally sequential in characteristic, a concurrent reaction model can have errors upon extrapolation outside the calibration interval.

A common model used in the fossil fuel arena is to mimic the reactivity distribution inherent in a heterogeneous material by using parallel reactions with a distribution of activation energies and the same frequency factor, or occasionally, a frequency factor that increases exponentially with activation energy. An isoconversional model would work just as well in this situation as long as baseline correction issues can be overcome. On the other hand, an issue that arises in fossil fuel conversion, polymer decomposition, and energetic material decomposition is that competition between the escape of intermediate products and their further reaction within the heated zone, either by themselves or with unreacted material, causes a different set of products depending on temperature and confinement conditions [20]. This situation is easily modeled, in principle, using traditional approaches, but it is not obvious how it can be modeled using the isoconversional approach.

Acknowledgements

This work was performed under the auspices of the U. S. Department of Energy by University of California, Lawrence Livermore National Laboratory, under Contract No. W-7405-Eng-48.

References

1 S. Vyazovkin, J. Comput. Chem., 22 (2001) 179.
2 H. L. Friedman, J. Polym. Sci., Part C, 6 (1964) 183.
3 T. J. Ozawa, J. Thermal Anal., 2 (1970) 301.
4 M. E. Brown, M. Maciejewski, S. Vyazovkin, R. Nomen, J. Sempere, A. Burnham, J. Opfermann, R. Strey, H. L. Anderson, A. Kemmler, R. Keuleers, J. Janssens, H. O. Desseyn, C.-R. Li, T. B. Tang, B. Roduit, J. Malek and T. Mitsuhashi, Thermochim. Acta, 355 (2000) 125.
5 A. K. Burnham, Thermochim. Acta, 355 (2000) 165.
6 A. K. Burnham and R. L. Braun, Energy Fuels, 13 (1999) 1.
7 B. Roduit, Ch. Borgeat, B. Berger, P. Folly, B. Alonso, J. N. Aebischer and F. Stoessel, J. Therm. Anal. Cal., 80 (2005) 229.
8 T. Akahira and T. Sunose, Res. Report Chiba Institute Technology, 16 (1971) 22.
9 J. H. Flynn and L. A. Wall, J. Polym. Sci., Part B, 4 (1966) 323.
10 T. Ozawa, Thermochim. Acta, 203 (1992) 159.
11 J. H. Flynn, Thermochim. Acta, 300 (1997) 83.
12 S. Vyazovkin and A. I. Lesnikovich, Russ. J. Phys. Chem., 62 (1988) 1535.
13 A. K. Burnham, J. Therm. Anal. Cal., 60 (2000) 895.
14 J. Šesták and G. Berggren, Thermochim. Acta, 3 (1971) 1.
15 R. L. Braun and A. K. Burnham, Energy Fuels, 1 (1987) 153.
16 E. G. Prout and F. C. Tompkins, Trans. Faraday Soc., 40 (1944) 488.
17 A. K. Burnham, R. L. Braun, H. R. Gregg and A. M. Samoun, Energy Fuels, 1 (1987) 452.
18 B. Roduit, C. Borgeat, B. Berger, P. Folly, B. Alonso and J. N. Aebischer, J. Therm. Anal. Cal., 80 (2005) 91.
19 M. J. Starink, Thermochim. Acta, 404 (2003) 163.
20 A. K. Burnham and R. K. Weese, Thermochim. Acta, 426 (2005) 85.

DOI: 10.1007/s10973-006-8486-1